IEEE Photonics Journal
An IEEE Photonics Society Publication

Constant Weight Space-Time Codes for Dimmable MIMO-VLC Systems

Volume 12, Number 6, December 2020

Jia-Ning Guo
Jian Zhang
Yan-Yu Zhang
Gang Xin
Lin Li

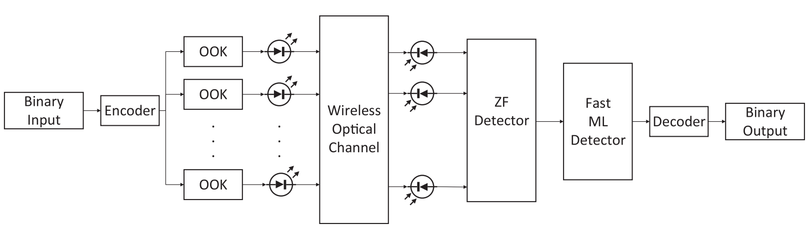

DOI: 10.1109/JPHOT.2020.3036648

IEEE photonics SOCIETY
IEEE

Constant Weight Space-Time Codes for Dimmable MIMO-VLC Systems

Jia-Ning Guo, Jian Zhang, Yan-Yu Zhang, Gang Xin, and Lin Li

National Digital Switching System Engineering and Technology Research Center,
Zhengzhou 450000, China

DOI:10.1109/JPHOT.2020.3036648

Manuscript received September 9, 2020; revised October 22, 2020; accepted November 3, 2020. Date of publication November 9, 2020; date of current version December 4, 2020. This work was supported in part by the Major Scientific and Technological of Henan Province, China under Grant 161100210200, in part by the Major Scientific and Technological of Guangdong Province, China under Grant 2016B010111001, in part by the National Key Research and Development Project (2018YFB1801903), and in part by the National Natural Science Foundation of China (NSFC) under Grants 62071489, 61671477, and 61901524. Corresponding author: Jian Zhang (e-mail: Zhang_xinda@126.com).

Abstract: Visible light communication(VLC), which combines communication and illumination, is regarded as a potential wireless communication. For illumination requirements of VLC systems, dimming control is a significant function. Many schemes have been proposed for multi-input multi-output (MIMO) VLC systems or dimmable VLC systems, but few schemes combine the two. The dimming control scheme that has been proposed for MIMO-VLC systems in the reference still has a probability for improvement in spectral efficiency and error performance. This paper proposes a dimming control scheme that utilizes the constant weight space-time codes (CWSTC) to improve spectral efficiency and error performance for MIMO-VLC systems. Simultaneously, we also present the codeword structure and a low implementation complexity detection algorithm for the scheme. Finally, performance analysis and simulation results provide comparisons between the proposed scheme and other existing dimming control schemes.

Index Terms: Visible light communication (VLC), dimming control, multi-input multi-output (MIMO), constant weight space-time codes (CWSTC).

1. Introduction

Visible light communication(VLC) is a potential kind of wireless communication with significant developments in recent years. VLC offers various advantages with higher data rates, license-free operation, and broadened spectrum than other wireless communications. The light-emitting diode (LED) is a new generation green lighting source with a long lifetime, small size, and low cost [1]. VLC utilizes extensive installed LEDs as the transmitters and uses intensity modulation and direct detection (IM/DD) to realize communication [2]. Because of the developments of the LED and the shortage of spectrum resources in traditional radio frequency (RF) communication, it is very urgent to research on VLC [3]–[5]. For that reason, a battery of standards for VLC has been proposed by IEEE [6].

As an integrated system with communication and illumination, VLC has more functions than other traditional wireless communications. Dimming control is a crucial function that can adjust the brightness according to users' demands [5]. Thus many dimming control schemes have been proposed for VLC systems. The essence of dimming control is to adjust the ratio of average power to peak power, which means we should adjust the average power when the peak power is fixed. Most of the dimming control schemes achieve dimming targets by coding and modulation. The methods and performance analysis of variable on-off keying (VOOK), variable pulse position modulation (VPPM), and multipulse pulse position modulation (MPPM) were introduced in [7]. Those schemes are modulation-based dimming control schemes that achieve the dimming targets by changing the modulation mode. Reed-Muller codes-based scheme [8], polar codes-based scheme[9], turbo codes-based scheme [10] and rate-compatible punctured convolutional (RCPC) code-based scheme [11] are the schemes based on coding that utilize channel coding and complementing bits to realize dimming control. Those schemes we mentioned above all are for single LED systems. They change the dimming factor by adjusting the ratio of '0' and '1' in the codewords and have excellent performance in the bit error rate (BER). However, the spectral efficiency is low due to a single transmitter. For this reason, many schemes for multi-LED systems have been proposed. Multilevel pulse amplitude modulation (ML-PAM) scheme [12], multilevel parity-check codes (ML-PCC) scheme [13] and variable pulse amplitude and position modulation (VPAPM) scheme [14] are representative schemes for multiple-input single-output (MISO) systems. Although these multi-LED dimming control schemes have improved spectral efficiency distinctly, there is still the possibility of further improvement. There are also many techniques and schemes proposed for multi-input multi-output (MIMO) VLC systems. Angle diversity techniques and optimized constellation design for MIMO-VLC systems are proposed in [15] and [16] respectively. However, both two schemes do not take into consideration the constraint of dimming control. Paper [17] proposed a scheme for uniform illumination, but the illumination consistency for every LED is not taken into account. Uniform illumination space-time codes (UISTC) scheme [18] is a dimming control scheme for MIMO systems. It can realize high data rate communication and achieve dimming targets, but the error performance and spectral efficiency are still likely to be improved. Thus in this paper, we provide a dimming control scheme based on constant weight space-time codes (CWSTC) for MIMO systems. The CWSTC scheme we proposed is applicable to general $N_t \times N_r$ MIMO-VLC systems as long as $N_r \geqslant N_t$, where N_r is the number of receivers and N_t is the number of transmitters. Such a constraint is to guarantee that the transmitted signal can be accurately recovered by the receiver. The proposed CWSTC scheme for $N_t \times N_r$ MIMO-VLC systems is slightly different from that for $N \times N$ MIMO-VLC systems. Therefore, in this paper, we first define the number of transmitters is N and introduce the CWSTC scheme applied to $N \times N$ MIMO-VLC systems and then present a supplementary explanation for the scheme applied to $N_t \times N_r$ MIMO-VLC systems. The proposed scheme has better spectral efficiency and BER performance than the UISTC scheme introduced in paper [18].

The other sections of this paper are organized as follows: Section. II proposes the system model of MIMO-VLC systems. Section. III introduces the codeword structure, the encoding algorithm, and the detection algorithm. The performance analysis and simulation results are presented in Section. IV. Section. V summarizes the contents of the whole paper.

2. System Model

The system model we proposed for the scheme consisting of N LED chips at the transmitter and N photo-detectors (PD) at the receiver. We assume that the direct light is dominant, and reflected light is negligible [3]. We assume the additive white Gaussian noise (AWGN) as the channel noise according to the model established in [3], [19]. Thus the received signal should be expressed as

$$\mathbf{Y} = \mathbf{H}\mathbf{X} + \mathbf{N}, \tag{1}$$

where $\mathbf{N}$ is the noise matrix of which the variance is σ^2, and the mean is 0. $\mathbf{H}$ is the channel gain matrix calculated by the Lambertian model that we will introduce below. $\mathbf{X}$ is the transmitted signal matrix, and $\mathbf{Y}$ is the received signal matrix with noise. All of the matrices we mentioned before are the $N \times N$ matrices. Based on the previously mentioned Lambertian model, the channel gain

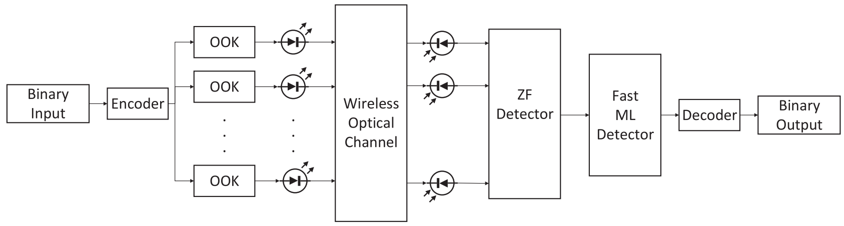

Fig. 1. System model of the proposed CWSTC scheme.

between the jth transmitter and the ith receiver is given as

$$h_{ij} = \begin{cases} \frac{A(m+1)}{2\pi D_{ij}^2} \cos^m(\phi_{ij}) T_S(\psi_{ij}) g(\psi_{ij}) \cos \psi_{ij}, & 0 \le \psi_{ij} \le \Psi_C \\ 0, & \psi_{ij} > \Psi_C \end{cases} \tag{2}$$

where m is the order of the Lambertian radiation which is determined by the half-power angle of the LED; A represents the physical area of PD at the receiver; ϕ_{ij} and ψ_{ij} denote the incidence angle and the irradiance angle; $T_S(\psi_{ij})$ and $g(\psi_{ij})$ are the optical filter gain and the concentrator gain respectively; D_{ij} is the distance between the jth transmitter and the ith receiver and Ψ_C denotes the field of view (FOV) of the PD.

In this paper, to realize dimming control, the peak power is fixed, and the average power can be changed to achieve dimming targets. Thus the dimming factor can be expressed as

$$\gamma = \frac{\bar{P}}{P}, \tag{3}$$

where P denotes the peak power, $\bar{P}$ is the average power, and γ represents the dimming factor with $0 < \gamma < 1$.

The system model of the proposed CWSTC scheme is shown in Fig. 1. When the binary data are coded by the encoder, a length-k binary data is mapped to a $N \times N$ transmitted signal matrix. The principles for the mapping are introduced in the next section. Then the transmitted signals are on-off keying (OOK) modulated and transmitted by the N transmitters in N time slots. After passing through the wireless optical channel, the received signals are detected successively by a zero-forcing (ZF) detector and a fast maximum likelihood (ML) detector. Then the output signal matrices would be decoded by the decoder. Finally, the system outputs the binary data. The codeword structure, the encoding algorithm, and the detection algorithm will be described in detail in the next section.

3. The Proposed Constant Weight Space-Time Codes Scheme

For the proposed CWSTC scheme, the number of transmitters N should be fixed. We assume there are N time slots in a period T. Thus, for every transmitter, each bit duration of the constant weight space-time codes is $T_s = T/N$. We suppose every k bits form a length-k binary vector and is uniquely mapped to a $N \times N$ code matrix. Thus we can transmit k bits in a period T utilizing the proposed scheme.

The codeword structure is shown in Fig. 2, where x_{jl} represents the bit transmitted by the jth transmitter in the lth time slot. Next, we will introduce the algorithms of encoding and detection.

3.1 Dimming Encoding of Constant Weight Space-Time Codes

The signal we prepare to transmit is a lot of binary bits. We divide the binary bits into many length-k binary vectors. Each vector is uniquely mapped to a space-time code with the structure in Fig. 2. We can regard a space-time code as a $N \times N$ square matrix. The dimming factor γ of the schemes

x_{11}	x_{12}	$\cdots$	$\cdots$	x_{1N}
x_{21}	x_{22}	$\cdots$	$\cdots$	x_{2N}
$\vdots$	$\vdots$	$\ddots$		$\vdots$
$\vdots$	$\vdots$		$\ddots$	$\vdots$
x_{N1}	x_{N2}	$\cdots$	$\cdots$	x_{NN}

Fig. 2. Codeword structure of the constant weight space-time codes.

Number of columns

Number of rows	1	2	3	......					N
1	0	N^0	$2\times N^0$	$\cdots$	$\cdots$	$\cdots$	$\cdots$	$\cdots$	$N^0(N-1)$
2	0	N^1	$2\times N^1$	$\cdots$	$\cdots$	$\cdots$	$\cdots$	$\cdots$	$N^1(N-1)$
3	0	N^2	$2\times N^2$	$\cdots$	$\cdots$	$\cdots$	$\cdots$	$\cdots$	$N^2(N-1)$
	0	$\vdots$	$\vdots$	$\cdots$	$\cdots$	$\cdots$	$\cdots$	$\cdots$	$\vdots$
......	0	$\vdots$	$\vdots$	$\cdots$	$\cdots$	$\cdots$	$\cdots$	$\cdots$	$\vdots$
	0	$\vdots$	$\vdots$	$\cdots$	$\cdots$	$\cdots$	$\cdots$	$\cdots$	$\vdots$
	0	$\vdots$	$\vdots$	$\cdots$	$\cdots$	$\cdots$	$\cdots$	$\cdots$	$\vdots$
N	0	$N^{(N-1)}$	$2\times N^{(N-1)}$	$\cdots$	$\cdots$	$\cdots$	$\cdots$	$\cdots$	$N^{(N-1)}(N-1)$

Fig. 3. Digit values represented by different positions in the square matrix.

based on space-time codes can be defined as [18].

$$\gamma = \frac{\text{Number of '1' s in the code matrix}}{\text{Number of bits in the code matrix}}, \tag{4}$$

To guarantee the uniqueness of the mapping and realize dimming control, each row of the matrix should have the same number of '1.' Thus when the number of transmitters N has been fixed, the dimming target the scheme can achieve is $1/N$, $2/N$, $3/N$, ..., and $(N-1)/N$. Next, we will introduce the encoding process when $\gamma = 1/N$. Other dimming factors can be achieved by changing the codes of $\gamma = 1/N$. Every bit '1' in different positions of the square matrix represents a different decimal digit value. The digit values represented by bit '1' in different positions in the square matrix is shown in Fig. 3. The digit value represented by a matrix is the summation of all the digit value that every bit '1' represents in the matrix. For example, when the $N = 3$ and the matrix is

$$\begin{bmatrix} 1 & 0 & 0 \\ 0 & 1 & 0 \\ 0 & 0 & 1 \end{bmatrix}$$

Thus the digit value that the matrix represents is $0 + N + 2N^2 = 21$.

By the structure of Fig. 3, we can express all integers from 0 to $N^N - 1$. To ensure the uniqueness of the mapping and maximize the spectral efficiency, the length of the binary vector k should satisfy the condition in Eq. (5)

$$k = \lfloor N \log_2 N \rfloor, \tag{5}$$

where $\lfloor \cdot p \rfloor$ denotes the downward rounding operation.

We present two examples of encoding when $\gamma = 1/N$ and $\gamma \neq 1/N$:

Example 1: We fixed $N = 4$ and the dimming target is $1/4$, thus the length of the divided vectors $k = 8$. When the binary data vector is [0, 0, 1, 1, 0, 1, 0, 1], we first convert the binary vector into a decimal digit value $s = 53$. Then we map s to the constant weight space-time code matrix utilizing the structure in Fig. 3. The corresponding space-time code matrix is

$$\begin{bmatrix} 0 & 1 & 0 & 0 \\ 0 & 1 & 0 & 0 \\ 0 & 0 & 0 & 1 \\ 1 & 0 & 0 & 0 \end{bmatrix}$$

Example 2: We fixed $N = 4$ and the dimming target is $3/4$, thus the length of the divided vectors $k = 8$. When the binary data vector is [0, 1, 0, 1, 0, 0, 1, 1], we first convert the binary vector into a decimal digit value $s = 83$. Then we map s to the constant weight space-time code matrix with $\gamma = 1/4$ utilizing the structure in Fig. 3. The corresponding space-time code matrix is

$$\begin{bmatrix} 0 & 0 & 0 & 1 \\ 1 & 0 & 0 & 0 \\ 0 & 1 & 0 & 0 \\ 0 & 1 & 0 & 0 \end{bmatrix}$$

Then we replace the two-bit ‘0’ on the right of the bit ‘1’ with ‘1.’ If the column number of the replacement exceeds N, start replacing it from the first column. Thus the corresponding space-time code matrix with $\gamma = 3/4$ is

$$\begin{bmatrix} 1 & 1 & 0 & 1 \\ 1 & 1 & 1 & 0 \\ 0 & 1 & 1 & 1 \\ 0 & 1 & 1 & 1 \end{bmatrix}$$

Algorithm. 1 summarizes the dimming encoding process.

From Fig. 3 and Algorithm. 1, we know that the code matrices of the CWSTC scheme can be mapped from 0 to $N^N - 1$. Thus when $N = 4$, the code matrices of the CWSTC scheme can be mapped from 0 to 255. For the sake of clear explanation and convenient presentation, we only provide the code matrices of the CWSTC scheme for mapping 0 to 15 for $N = 4$ with $\gamma = 0.25$, $\gamma = 0.5$, and $\gamma = 0.75$. The code matrices are postponed to Appendix A.

3.2 Dimming Detection of Constant Weight Space-Time Codes

For the proposed CWSTC dimming control scheme, the traditional Maximum Likelihood (ML) detection algorithm has the best performance. It utilizes the probability density function of $\mathbf{Y}$ under $\mathbf{HX}$ conditions, which can be expressed as

$$p(\mathbf{Y}|\mathbf{HX}) = \frac{1}{(\sqrt{2\pi\sigma^2})^N} \exp\left(-\frac{\|\mathbf{Y} - \mathbf{HX}\|^2}{2\sigma^2}\right). \tag{6}$$

Algorithm 1: Constant Weight Space-Time Encoding.

Input:The dimming factor γ, the number of transmitters N and the divided length-k input data bit $\mathbf{b}_k$
  Convert the length-k binary vector $\mathbf{b}_k$ into a decimal digital value s
  For $i = N : -1 : 1$
    For $m = 1 : N$
      $p = 0$
      a is the number represented by the coordinate (i, m) in Fig. 3
      If $p \leqslant a \leqslant s$
        $p = a,\ j = m$
      End
    End
    $s = s - p$
    $\mathbf{X}(i, j) = 1$ and the other elements in the ith row is 0.
    If $\gamma = \frac{M}{N}$ and $M \neq 1$
      For n=1:M-1
        $\mathbf{X}(i, j \oplus n) = 1$, where $\oplus$ denotes the $(N+1)$-ary addition
      End
    End
  End
Output:The transmitted space-time code matrix $\mathbf{X}$

Under the equiprobable input condition, the ML detector equals the minimum Euclidean distance (MED) detector, and it can be given by

$$\hat{\mathbf{X}}_{ML} = \arg\min \|\mathbf{Y} - \mathbf{H}\mathbf{X}\|^2, \tag{7}$$

where $\hat{\mathbf{X}}_{ML}$ is the estimated matrix by MED detector of the transmitted space-time code. The essence of the MED detector is to search for Euclidean distance between the received signal with noise $\mathbf{Y}$ and the equivalent transmitted signal $\mathbf{HX}$ exhaustively. The complexity of this algorithm is $O(2^{N^2})$, and it is too high to implement in practice.

In this paper, we provide another detection algorithm, which consists of three parts: Zero-forcing (ZF) detection, fast maximum likelihood (ML) detection, and CWSTC decoding. The received signal $\mathbf{Y}$ is detected by the ZF detector, which can be given by

$$\hat{\mathbf{X}}_{ZF} = \mathbf{H}^{-1}\mathbf{Y}, \tag{8}$$

where $\mathbf{H}^{-1}$ represents the inverse of the channel gain matrix $\mathbf{H}$.

To facilitate the calculation of Euclidean distance between two matrices, we convert the $N \times N$ matrix into a $1 \times N^2$ vector. Thus the ML detector can be expressed as

$$\hat{\mathbf{x}} = \arg\min \|\mathbf{r} - \mathbf{x}\|^2, \tag{9}$$

where $\hat{\mathbf{x}}$ is the $1 \times N^2$ ultimate estimated vector, $\mathbf{r}$ represents the converted vector of $\hat{\mathbf{X}}_{ZF}$ and $\mathbf{x}$ denotes the converted vector of $\mathbf{X}$.

For the vectors $\mathbf{r}$ and $\mathbf{x}$, the Euclidean distance can also be represented as

$$\|\mathbf{r} - \mathbf{x}\|^2 = \|\mathbf{r}\|^2 + \|\mathbf{x}\|^2 - 2\mathbf{r}^T\mathbf{x}, \tag{10}$$

where $\|\mathbf{r}\|^2 = \sum_{i=1}^{N^2} r_i$ is a constant for a certain vector $\mathbf{r}$ and $\|\mathbf{x}\|^2 = \sum_{i=1}^{N^2} x_i$ is also a constant because the space-time codes are constant weight. Combined (9) and (10) the ML detector can also be represented as

$$\hat{\mathbf{x}} = \arg\min(-2\mathbf{r}^T\mathbf{x}) = \arg\max \mathbf{r}^T\mathbf{x}. \tag{11}$$

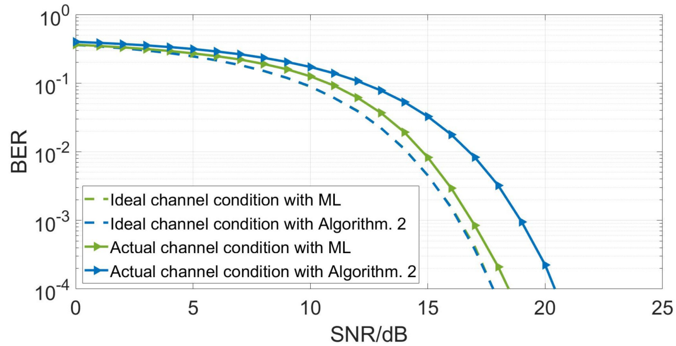

Fig. 4. Comparison between ML detection algorithm and the proposed algorithm.

Algorithm 2: Constant Weight Space-Time Detection.

Input:The dimming factor γ, the number of transmitters N and the received signal matrix $\mathbf{Y}$
Zero forcing (ZF) detection: $\hat{\mathbf{X}}_{ZF} = \mathbf{H}^{-1}\mathbf{Y}$
Convert $N \times N$ matrices $\hat{\mathbf{X}}_{ZF}$ and all of the space-time codes $\mathbf{X}$ to $1 \times N^2$ vectors $\mathbf{r}$ and $\mathbf{x}$ respectively.
Find all positions of bit '1' in $\mathbf{x}$ and sum up all elements in $\mathbf{r}$ at the same position to get the summation S.
$\hat{\mathbf{x}} = \arg\max \mathbf{r}^T\mathbf{x} = \arg\max S$
Convert $1 \times N^2$ vector $\hat{\mathbf{x}}$ into $N \times N$ matrix $\hat{\mathbf{X}}$
If $\gamma = \frac{M}{N}$ and $M \neq 1$
  For i=1:N
    Find the number j which is the column number of the first bit '0' in the ith row.
    For i=1:M-1
      $\hat{\mathbf{X}}(i, j \ominus n) = 0$, where $\ominus$ denotes the $(N+1)$-ary subtraction.
    End
  End
End
Calculate the decimal digital value $\hat{s}$ which the $N \times N$ matrix $\hat{\mathbf{X}}$ represents by utilizing Fig. 3
Convert the decimal digital value $\hat{s}$ into length-k binary vector $\hat{b}_k$
Output:The estimated length-k binary vector $\hat{b}_k$

We know that $\mathbf{x}$ is the vector consists of '0' and '1.' Thus we should find all positions of bit '1' in $\mathbf{x}$ and sum up all elements in $\mathbf{r}$ at the same position. For example, if $\mathbf{x} = (0, 1, 1, 0)$ and $\mathbf{r} = (0.21, 1.07, 0.95, 0.4)$, we first find the positions of bit '1' in $\mathbf{x}$ is the second one and the third one, then we sum up all elements in $\mathbf{r}$ at the same position $S = \mathbf{r}^T\mathbf{x} = 1.07 + 0.95 = 3.02$. Thus we can compare all the summations to achieve the ultimate estimated vector $\hat{\mathbf{x}}$. At last, we convert $\hat{\mathbf{x}}$ to the matrix $\hat{\mathbf{X}}$ and map it to the binary data. The Algorithm. 2. summarizes the detection algorithm.

Analysis indicates that the complexity of the detection algorithm we proposed is mainly from searching for the positions of bit '1.' Thus the complexity is $O(N^2)$. The simulation result of Algorithm. 2 is shown in Fig. 4. We compare the ML detection algorithm and the proposed Algorithm. 2 under ideal channel condition and actual channel condition. The ideal channel condition is the channel condition without inter-channel interference. We can see that the two algorithms have the same error performance under the ideal channel condition. Under the actual channel condition, the proposed Algorithm. 2 is worse than the ML detection algorithm. Although there will be a bit loss of error performance due to ZF detection, the reduction of complexity makes the scheme convenient for practical application. We can reduce inter-channel interference through other techniques to achieve better error performance.

When the MIMO-VLC system contains N_r receivers and N_t transmitters, in Eq. (1), the code matrix $\mathbf{X}$ is a $N_t \times N_t$ matrix, the channel gain matrix $\mathbf{H}$ is a $N_r \times N_t$ matrix, and the noise matrix $\mathbf{N}$ is a $N_r \times N_t$ matrix. Thus the received signal matrix with noise $\mathbf{Y}$ is also a $N_r \times N_t$ matrix. When the channel gain matrix $\mathbf{H}$ is a $N_r \times N_t$ matrix, in Eq. (8), $\mathbf{H}^{-1}$ is a $N_t \times N_r$ matrix which represents the pseudo-inverse matrix of $\mathbf{H}$. Therefore, the output of the ZF detector $\hat{\mathbf{X}}_{ZF}$ is a $N_t \times N_t$ matrix. The other steps of coding and detection are the same as that of the $N \times N$ MIMO-VLC system.

4. Performance Analysis and Simulation Results

This section will present the performance analysis and simulation results, including run-length, spectral efficiency, normalized power requirement, minimum Euclidean distance, and error performance of the proposed CWSTC scheme.

As the main contrast scheme, the UISTC scheme is also proposed for dimmable MIMO-VLC systems. The code matrix of the UISTC scheme strictly guarantees the same number of bit '1' in every time slot while ensuring the dimming control constraint. The position of bit '1' in each row of the UISTC code matrix can be achieved by iterative computations provided in [18]. Compared with the CWSTC scheme we proposed, the UISTC scheme focuses more on the uniformity of illumination in each time slot and has higher encoding/decoding complexity.

The system model of the dimming control scheme we proposed includes N LEDs as transmitters. They work together to transmit the signals. We regard them as a whole illumination system. From the content in [20], we know that the human sensitivity on frequency relied on the modulation depth. That means when the modulation depth is fixed, and the intensity of illumination changes faster than a specific frequency, the human eye senses the average illumination rather than the instantaneous intensity. The modulation depth of OOK modulation is 100% [21], and run-length limitation can guarantee the intensity of illumination changes faster than the specific frequency. Therefore, for the dimmable VLC system proposed in this paper, it is unnecessary to be strictly dimming uniform for every time slot. We only need to pay attention to guarantee the average illumination intensity rather than the instantaneous intensity in every time slot.

4.1 Run-Length

In the VLC system, run-length is the number of continuous bits ('0' or '1') of a transmitter. For the sake of flicker mitigation, run-length should be limited. Paper [22] proposed a run-length limited code that can decrease error, achieve the dimming target, and avoid flicker. Many dimming control schemes take into consideration run-length limitation such as [18], [23] and [24]. Thus run-length limitation is essential for dimmable VLC systems.

The human sensitivity on frequency relied on the modulation depth. From Fig. 18 in [20], we know that when the flicker frequency is greater than 90 Hz, the recommended low-risk region can be expressed as

$$\mathcal{M} \leqslant 0.08 \times f, \tag{12}$$

where $\mathcal{M}\%$ is the Michelson contrast which is also known as modulation depth and f represents the frequency of driving current [20]. From Fig. 1 in Section. II, we can see that the proposed scheme utilizes OOK modulation. The modulation depth of OOK modulation is 100% [21]. When we substitute $\mathcal{M} = 100$ into Eq. (12), the lowest frequency of the recommended low-risk region f_{lowest} is 1.25 kHz. It means when $f \geqslant f_{\text{lowest}}$, the proposed CWSTC scheme can avoid flicker. The lowest optical clock frequency of the IEEE VLC standard is 200 kHz, which can be expressed as $f_{LOC} = 200$ kHz [6]. Thus the number of transmitters N should satisfy the following constraint.

$$\frac{(2N-2)}{f_{LOC}} \leqslant \frac{1}{f_{\text{lowest}}}. \tag{13}$$

We substitute $f_{LOC} = 200$ kHz and $f_{\text{lowest}} = 1.25$ kHz into Eq. (13) and the result is $N \leqslant 81$. If N is not greater than 81, the run-length is limited, and the LEDs in the VLC system can avoid flicker.

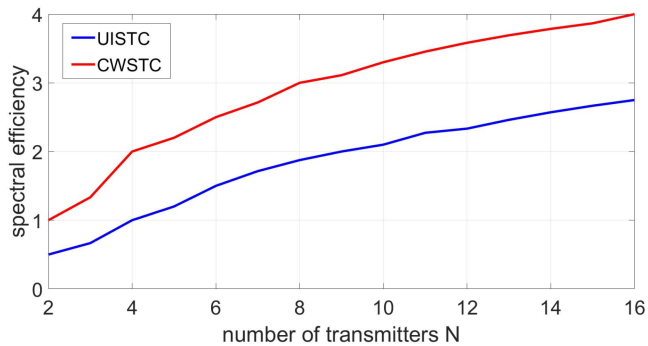

Fig. 5. Spectral efficiency of UISTC and CWSTC.

4.2 Spectral Efficiency

Spectral efficiency is a significative index for communication systems. It indicates the effective bit rate R_b can be realized when the bandwidth B is fixed. Based on the definition in [7], the spectral efficiency of the CWSTC scheme can be defined as

$$\nu_{CWSTC} = \frac{R_{b-CWSTC}}{B} = \frac{R_{b-CWSTC}}{\frac{1}{T_s}} = \frac{\frac{\lfloor N \log_2 N \rfloor}{NT_s}}{\frac{1}{T_s}} = \frac{\lfloor N \log_2 N \rfloor}{N}, \tag{14}$$

where $R_{b-CWSTC}$ is the bit rate of the CWSTC scheme.

From the Eq. (14), we know that the spectral efficiency of the CWSTC scheme only relates to the number of transmitters N, unlike the schemes introduced in [7], [13], and [24], the spectral efficiency of which relates to the dimming factor γ. Thus in this paper, for convenience and fairness, we compare the CWSTC scheme with the UISTC scheme proposed in [18]. The spectral efficiency of the UISTC scheme can be given as

$$\nu_{UISTC} = \frac{R_{b-UISTC}}{B} = \frac{R_{b-UISTC}}{\frac{1}{T_s}} = \frac{\frac{\lfloor \log_2 N! \rfloor}{NT_s}}{\frac{1}{T_s}} = \frac{\lfloor \log_2 N! \rfloor}{N}, \tag{15}$$

where $R_{b-UISTC}$ is the bit rate of the UISTC scheme.

From Eq. (14) and Eq. (15), we can intuitively see that the CWSTC scheme has higher spectral efficiency than the UISTC scheme. That is because the CWSTC scheme expands the codewords set compared with the UISTC scheme, and the expansion results in the increase of the bit rate. The comparison is shown in Fig. 5.

From Fig. 5, we can see that the spectral efficiency of the CWSTC scheme is higher than the UISTC scheme when N is fixed. The CWSTC scheme focuses on the average illumination intensity rather than the instantaneous intensity in every time slot. The cardinality of the CWSTC codewords set $\mathcal{B}_{CWSTC}$ is N^N while the cardinality of the UISTC codewords set $\mathcal{B}_{UISTC}$ is $N!$. When N is an integer greater than 1, the cardinality of $\mathcal{B}_{CWSTC}$ is greater than that of $\mathcal{B}_{UISTC}$. Thus, there is a big gap between the two schemes in spectral efficiency.

4.3 Normalized Power Requirement

Normalized power requirement is an index representing the power required to achieve a given bit error rate when the bit rate is fixed. For the sake of fair comparison, we choose some multi-LED dimming control schemes as the contrasts. First, we should present the transmitted optical signal

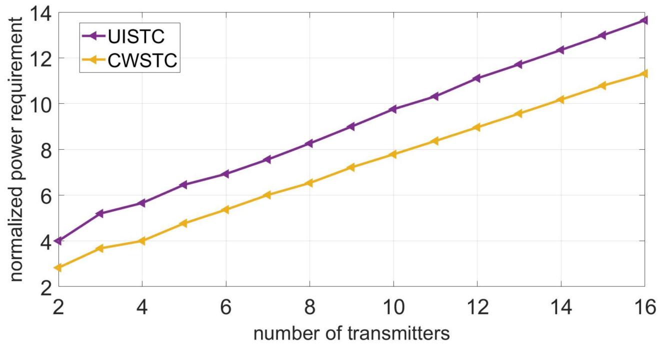

Fig. 6. Normalized power requirements of UISTC and CWSTC.

equation of the proposed CWSTC, which is

$$x(t) = \frac{P}{N}\sum_{j=1}^{N}\sum_{l=1}^{N} x_{j,l}\, rect\left(\frac{Nt}{T} - l\right), \tag{16}$$

where P denotes the peak power, $x_{j,l}$ represents the bit in Fig. 2 which is the bit transmitted from the jth transmitter in the lth time slot. When we calculate the normalized power requirement, the OOK scheme is the baseline scheme. Thus the normalized power requirement of the CWSTC scheme can be expressed as

$$P_{CWSTC} \approx \frac{d_{OOK}}{d_{CWSTC}} P_{OOK}, \tag{17}$$

where $d_{OOK} = \frac{2P}{\sqrt{R_b}}$ [7].

We then calculate the minimum Euclidean distance of the proposed CWSTC scheme when the peak power P is fixed by the method mentioned in [7]. The MED between two signals of the CWSTC scheme is

$$d_{CWSTC} = \frac{P}{N}\sqrt{\frac{2\lfloor N\log_2 N\rfloor}{NR_b}}. \tag{18}$$

When we substitute Eq. (18) into Eq. (17), we can achieve the normalized power requirement of the proposed scheme, which is expressed as

$$P_{CWSTC} = N\sqrt{\frac{2N}{\lfloor N\log_2 N\rfloor}}. \tag{19}$$

Fig. 6 presents the normalized power requirements of the UISTC scheme and the CWSTC scheme. We can see that the normalized power requirement of the CWSTC scheme is better than that of the UISTC scheme with the same N.

Note that unlike ML-MPPM and ML-ICWC, the normalized power requirement of the proposed scheme and the UISTC scheme only depends on the number of transmitters N. Thus the MED and the normalized power requirement are constant when N is fixed. Fig. 7 presents the normalized power requirements of the proposed scheme and other multi-LED schemes when $N = 4$ and $N = 8$.

From Fig. 7, we can see that the normalized power requirement of the CWSTC scheme is not only better than the UISTC scheme but also other multi-LED dimming control schemes. That is all due to the MIMO-VLC construction and the constant weight space-time codes make use of space resources.

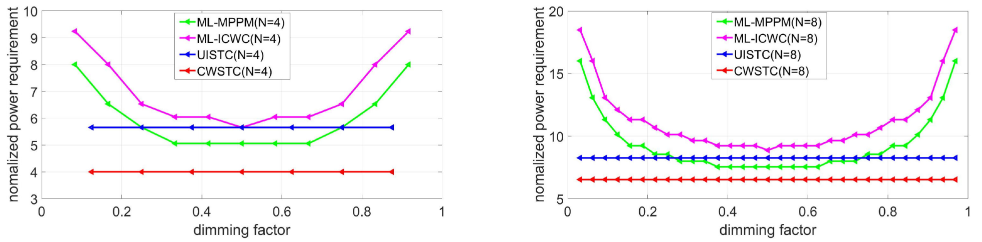

(a) Normalized power requirements with $N = 4$ (b) Normalized power requirements with $N = 8$

Fig. 7. Normalized power requirements of ML-MPPM, ML-ICWC, UISTC, and CWSTC with $N = 4$ and $N = 8$.

4.4 Minimum Euclidean Distance

In the previous subsection, we calculate the minimum Euclidean distance and normalized power requirement of the transmitted signal. For MIMO-VLC systems, the MED of the received signals is more critical. It directly determines the error performance of a MIMO-VLC system. Thus in this subsection, the MED between received signals for the proposed CWSTC scheme is derived and compared with that for the UISTC scheme.

First we define signal matrix without noise at the receiver is

$$\mathbf{R} = \mathbf{HX} = \begin{bmatrix} r_{11} & r_{12} & \cdots & r_{1N} \\ r_{21} & r_{22} & \cdots & r_{2N} \\ \vdots & \vdots & \ddots & \vdots \\ r_{N1} & r_{N2} & \cdots & r_{NN} \end{bmatrix}, \tag{20}$$

$$r_{il} = h_{i1}x_{1l} + h_{i2}x_{2l} + \cdots + h_{iN}x_{Nl} = \sum_{j=1}^{N} h_{ij}x_{jl}, \tag{21}$$

where r_{il} represents the signal received by the ith receiver in the lth time slot.

According to the form of Eq. (16), we provide the equation of received optical signal without noise that can be summarized as

$$r(t) = \frac{P}{N}\sum_{i=1}^{N}\sum_{l=1}^{N} r_{il}\, rect\left(\frac{Nt}{T} - l\right). \tag{22}$$

Then we present the equation of the MED of the received signal which can be expressed as

$$d_{R-CWSTC} = \sqrt{\int_0^T \|r^a(t) - r^b(t)\|^2 dt}, \tag{23}$$

where $r^a(t)$ and $r^b(t)$ are the two received signals with minimum Euclidean distance.

When we substitute Eq. (21) and Eq. (22) into Eq. (23), we have

$$d_{R-CWSTC} = \frac{P}{N}\sqrt{\int_0^T \|\sum_{i=1}^{N}\sum_{l=1}^{N}\sum_{j=1}^{N} h_{ij}(x_{jl}^a - x_{jl}^b)\, rect\left(\frac{Nt}{T} - l\right)\|^2 dt}, \tag{24}$$

where x_{jl}^a and x_{jl}^b are the elements of matrix $\mathbf{X}^a$ and matrix $\mathbf{X}^b$.

We combine the codeword structure with the definition of integral and simplify the Eq. (24). The MED of the received signal can be expressed as

$$d_{R-CWSTC} = \frac{P}{N}\sqrt{2T_s \| \sum_{j=1}^{N} h_{ij}(x_{jl}^a - x_{jl}^b)\|^2} = \frac{P}{N}\sqrt{\frac{2\lfloor N\log_2 N\rfloor}{NR_b}\| \sum_{j=1}^{N} h_{ij}(x_{jl}^a - x_{jl}^b)\|^2}, \quad (25)$$

where $T_s = T/N$ represents the bit period and '2' in Eq. (25) is the minimum number of different elements between matrix $\mathbf{X}^a$ and matrix $\mathbf{X}^b$. The minimum number is '2' because the code weight of the proposed codes is constant. We know that x_{jl}^a and x_{jl}^b are '0' or '1'. Thus the value of $(x_{jl}^a - x_{jl}^b)$ is 0 or ± 1. We can divide Eq. (25) into two situations:

1) The two different elements between matrix $\mathbf{X}^a$ and matrix $\mathbf{X}^b$ are in the same column. The MED can be denoted as $d_{R-CWSTC} = \frac{P}{N}\sqrt{\frac{2\lfloor N\log_2 N\rfloor}{NR_b}\min\{(h_{mn} - h_{mp})^2\}}$, where h_{mn} and h_{mp} represent the different elements in the same row of the channel gain matrix $\mathbf{H}$.
2) The two different elements between matrix $\mathbf{X}^a$ and matrix $\mathbf{X}^b$ are not in the same column. The MED can be denoted as $d_{R-CWSTC} = \frac{P}{N}\sqrt{\frac{2\lfloor N\log_2 N\rfloor}{NR_b}\min\{(h_{mn} + h_{pq})^2\}}$, where h_{mn} and h_{pq} represent the elements in different row of the channel gain matrix $\mathbf{H}$.

Thus the MED of the received signal for the CWSTC scheme is expressed as

$$d_{R-CWSTC} = \min\left[\frac{P}{N}\sqrt{\frac{2\lfloor N\log_2 N\rfloor}{NR_b}\min\{(h_{mn} - h_{mp})^2\}}, \frac{P}{N}\sqrt{\frac{2\lfloor N\log_2 N\rfloor}{NR_b}\min\{(h_{mn} + h_{pq})^2\}}\right]. \quad (26)$$

In the same way, we can achieve the MED of the received signal for the UISTC scheme is

$$d_{R-UISTC} = \min\left[\frac{P}{N}\sqrt{\frac{2\lfloor \log_2 N!\rfloor}{NR_b}\min\{(h_{mn} - h_{mp})^2\}}, \frac{P}{N}\sqrt{\frac{2\lfloor \log_2 N!\rfloor}{NR_b}\min\{(h_{mn} + h_{pq})^2\}}\right]. \quad (27)$$

It is not hard to conclude that with the same channel gain matrix $\mathbf{H}$, $d_{R-CWSTC} \geqslant d_{R-UISTC}$ when $N \geqslant 2$. Thus we can also conclude that the error performance of the CWSTC scheme is better than that of the UISTC scheme under the same channel conditions. The simulation result is shown in the next subsection.

4.5 Error Performance

Error performance is usually expressed by the curve of bit error rate (BER). The curve reflects the relation between BER and signal-to-noise ratio (SNR). The SNR can be expressed as

$$\mathrm{SNR} = 10\lg\frac{1}{R_C\sigma^2}, \quad (28)$$

where R_C denotes the code rate. Thus we can fairly compare different dimming control schemes.

In this subsection, we compare the error performance of the CWSTC scheme with the UISTC scheme under different channel conditions. Different positions of the transmitters and receivers lead to different channel conditions. Thus we present two different channel conditions. We normalize the channel gain without loss of generality [25], and the channel conditions are

$$\mathbf{H_1} = \begin{bmatrix} 1 & 0.364 & 0.291 & 0.301 \\ 0.289 & 0.954 & 0.315 & 0.298 \\ 0.295 & 0.312 & 0.975 & 0.345 \\ 0.354 & 0.297 & 0.356 & 0.96 \end{bmatrix}, \mathbf{H_2} = \begin{bmatrix} 0.517 & 0.417 & 0.409 & 0.401 \\ 0.393 & 0.686 & 0.420 & 0.396 \\ 0.397 & 0.395 & 0.652 & 0.403 \\ 0.415 & 0.413 & 0.398 & 0.550 \end{bmatrix}$$

We calculate $cond(\mathbf{H_1}) = 3.194$ and $cond(\mathbf{H_2}) = 14.7359$ which means the spatial correlation of $\mathbf{H_2}$ is more higher than $\mathbf{H_1}$. The simulation results are shown in Fig. 8.

From Fig. 8, we know that under the same channel conditions, the error performance of the CWSTC scheme is better than that of the UISTC scheme regardless of the spatial correlation. That

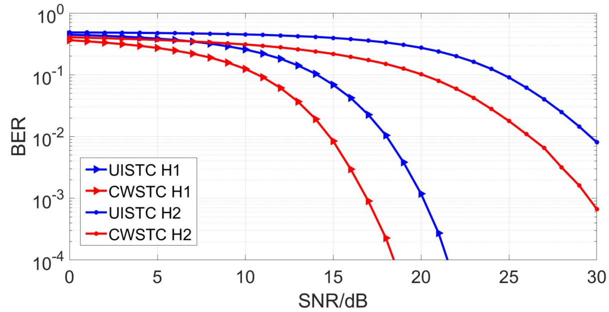

Fig. 8. Error performance of UISTC and CWSTC.

is because the MED between the received optical signals of the CWSTC is greater under the same channel condition. We can also see that as the spatial correlation becomes higher, the inter-channel interference increases. Therefore, the two schemes' error performance becomes worse.

5. Conclusion

In this paper, we proposed a CWSTC dimming control scheme that can realize data transmission and illumination for MIMO-VLC systems. We also provide an encoding algorithm and a fast dimming detection algorithm to reduce complexity. By performance analysis, the run-length limitation of the codes can avoid flicker, and the minimum Euclidean distance between the received signals of the proposed scheme is greater than that of the existing scheme. From simulation results, the proposed scheme has higher spectral efficiency and better error performance compared with others. Therefore, the proposed CWSTC scheme can be an attractive choice for MIMO-VLC systems to achieve dimming targets.

Appendix A

The code matrices for mapping 0 to 15 for $N = 4$ with $\gamma = 0.25$ are as follows:

$$\begin{bmatrix}1&0&0&0\\1&0&0&0\\1&0&0&0\\1&0&0&0\end{bmatrix},\begin{bmatrix}0&1&0&0\\1&0&0&0\\1&0&0&0\\1&0&0&0\end{bmatrix},\begin{bmatrix}0&0&1&0\\1&0&0&0\\1&0&0&0\\1&0&0&0\end{bmatrix},\begin{bmatrix}0&0&0&1\\1&0&0&0\\1&0&0&0\\1&0&0&0\end{bmatrix},\begin{bmatrix}1&0&0&0\\0&1&0&0\\1&0&0&0\\1&0&0&0\end{bmatrix},$$

$$\begin{bmatrix}0&1&0&0\\0&1&0&0\\1&0&0&0\\1&0&0&0\end{bmatrix},\begin{bmatrix}0&0&1&0\\0&1&0&0\\1&0&0&0\\1&0&0&0\end{bmatrix},\begin{bmatrix}0&0&0&1\\0&1&0&0\\1&0&0&0\\1&0&0&0\end{bmatrix},\begin{bmatrix}1&0&0&0\\0&0&1&0\\1&0&0&0\\1&0&0&0\end{bmatrix},\begin{bmatrix}0&1&0&0\\0&0&1&0\\1&0&0&0\\1&0&0&0\end{bmatrix},$$

$$\begin{bmatrix}0&0&1&0\\0&0&1&0\\1&0&0&0\\1&0&0&0\end{bmatrix},\begin{bmatrix}0&0&0&1\\0&0&1&0\\1&0&0&0\\1&0&0&0\end{bmatrix},\begin{bmatrix}1&0&0&0\\0&0&0&1\\1&0&0&0\\1&0&0&0\end{bmatrix},\begin{bmatrix}0&1&0&0\\0&0&0&1\\1&0&0&0\\1&0&0&0\end{bmatrix},\begin{bmatrix}0&0&1&0\\0&0&0&1\\1&0&0&0\\1&0&0&0\end{bmatrix},\begin{bmatrix}0&0&0&1\\0&0&0&1\\1&0&0&0\\1&0&0&0\end{bmatrix}.$$

The code matrices for mapping 0 to 15 for $N = 4$ with $\gamma = 0.5$ are as follows:

$$\begin{bmatrix}1&1&0&0\\1&1&0&0\\1&1&0&0\\1&1&0&0\end{bmatrix}, \begin{bmatrix}0&1&1&0\\1&1&0&0\\1&1&0&0\\1&1&0&0\end{bmatrix}, \begin{bmatrix}0&0&1&1\\1&1&0&0\\1&1&0&0\\1&1&0&0\end{bmatrix}, \begin{bmatrix}1&0&0&1\\1&1&0&0\\1&1&0&0\\1&1&0&0\end{bmatrix}, \begin{bmatrix}1&1&0&0\\0&1&1&0\\1&1&0&0\\1&1&0&0\end{bmatrix},$$

$$\begin{bmatrix}0&1&1&0\\0&1&1&0\\1&1&0&0\\1&1&0&0\end{bmatrix}, \begin{bmatrix}0&0&1&1\\0&1&1&0\\1&1&0&0\\1&1&0&0\end{bmatrix}, \begin{bmatrix}1&0&0&1\\0&1&1&0\\1&1&0&0\\1&1&0&0\end{bmatrix}, \begin{bmatrix}1&1&0&0\\0&0&1&1\\1&1&0&0\\1&1&0&0\end{bmatrix}, \begin{bmatrix}0&1&1&0\\0&0&1&1\\1&1&0&0\\1&1&0&0\end{bmatrix},$$

$$\begin{bmatrix}0&0&1&1\\0&0&1&1\\1&1&0&0\\1&1&0&0\end{bmatrix}, \begin{bmatrix}1&0&0&1\\0&0&1&1\\1&1&0&0\\1&1&0&0\end{bmatrix}, \begin{bmatrix}1&1&0&0\\1&0&0&1\\1&1&0&0\\1&1&0&0\end{bmatrix}, \begin{bmatrix}0&1&1&0\\1&0&0&1\\1&1&0&0\\1&1&0&0\end{bmatrix}, \begin{bmatrix}0&0&1&1\\1&0&0&1\\1&1&0&0\\1&1&0&0\end{bmatrix}, \begin{bmatrix}1&0&0&1\\1&0&0&1\\1&1&0&0\\1&1&0&0\end{bmatrix}.$$

The code matrices for mapping 0 to 15 for $N = 4$ with $\gamma = 0.75$ are as follows:

$$\begin{bmatrix}1&1&1&0\\1&1&1&0\\1&1&1&0\\1&1&1&0\end{bmatrix}, \begin{bmatrix}0&1&1&1\\1&1&1&0\\1&1&1&0\\1&1&1&0\end{bmatrix}, \begin{bmatrix}1&0&1&1\\1&1&1&0\\1&1&1&0\\1&1&1&0\end{bmatrix}, \begin{bmatrix}1&1&0&1\\1&1&1&0\\1&1&1&0\\1&1&1&0\end{bmatrix}, \begin{bmatrix}1&1&1&0\\0&1&1&1\\1&1&1&0\\1&1&1&0\end{bmatrix}, \begin{bmatrix}0&1&1&1\\0&1&1&1\\1&1&1&0\\1&1&1&0\end{bmatrix},$$

$$\begin{bmatrix}1&0&1&1\\0&1&1&1\\1&1&1&0\\1&1&1&0\end{bmatrix}, \begin{bmatrix}1&1&0&1\\0&1&1&1\\1&1&1&0\\1&1&1&0\end{bmatrix}, \begin{bmatrix}1&1&1&0\\1&0&1&1\\1&1&1&0\\1&1&1&0\end{bmatrix}, \begin{bmatrix}0&1&1&1\\1&0&1&1\\1&1&1&0\\1&1&1&0\end{bmatrix}, \begin{bmatrix}1&0&1&1\\1&0&1&1\\1&1&1&0\\1&1&1&0\end{bmatrix}, \begin{bmatrix}1&1&0&1\\1&0&1&1\\1&1&1&0\\1&1&1&0\end{bmatrix},$$

$$\begin{bmatrix}1&1&1&0\\1&1&0&1\\1&1&1&0\\1&1&1&0\end{bmatrix}, \begin{bmatrix}0&1&1&1\\1&1&0&1\\1&1&1&0\\1&1&1&0\end{bmatrix}, \begin{bmatrix}1&0&1&1\\1&1&0&1\\1&1&1&0\\1&1&1&0\end{bmatrix}, \begin{bmatrix}1&1&0&1\\1&1&0&1\\1&1&1&0\\1&1&1&0\end{bmatrix}.$$

References

[1] H. Le Minh *et al.*, "100-mb/s NRZ visible light communications using a postequalized white LED," *IEEE Photon. Technol. Lett.*, vol. 21, no. 15, pp. 1063–1065, Aug. 2009.

[2] D. Karunatilaka, F. Zafar, V. Kalavally, and R. Parthiban, "LED based indoor visible light communications: State of the art," *IEEE Commun. Surveys Tuts.*, vol. 17, no. 3, pp. 1649–1678, Jul.–Sep. 2015.

[3] T. Komine and M. Nakagawa, "Fundamental analysis for visible-light communication system using LED lights," *IEEE Trans. Consum. Electron.*, vol. 50, no. 1, pp. 100–107, Feb. 2004.

[4] H. Elgala, R. Mesleh, and H. Haas, "Indoor optical wireless communication: Potential and state-of-the-art," *IEEE Commun. Mag.*, vol. 49, no. 9, pp. 56–62, Sep. 2011.

[5] S. Rajagopal, R. D. Roberts, and S. Lim, "IEEE 802.15.7 visible light communication: Modulation schemes and dimming support," *IEEE Commun. Mag.*, vol. 50, no. 3, pp. 72–82, Mar. 2012.

[6] *IEEE Draft Standard for Local and Metropolitan Area Networks - Part 15.7: Short-Range Opt. Wireless Commun.*, IEEE P802.15.7/D3, Aug. 2018, pp. 1–412, 2018.

[7] K. Lee and H. Park, "Modulations for visible light communications with dimming control," *IEEE Photon. Technol. Lett.*, vol. 23, no. 16, pp. 1136–1138, Aug. 2011.

[8] S. Kim and S. Jung, "Novel FEC coding scheme for dimmable visible light communication based on the modified Reed-Muller codes," *IEEE Photon. Technol. Lett.*, vol. 23, no. 20, pp. 1514–1516, Oct. 2011.

[9] J. Fang *et al.*, "An efficient flicker-free FEC coding scheme for dimmable visible light communication based on polar codes," *IEEE Photon. J.*, vol. 9, no. 3, Jun. 2017, Art. no. 7903310.

[10] S. H. Lee and J. K. Kwon, "Turbo code-based error correction scheme for dimmable visible light communication systems," *IEEE Photon. Technol. Lett.*, vol. 24, no. 17, pp. 1463–1465, Sep. 2012.

[11] J. Kim and H. Park, “A coding scheme for visible light communication with wide dimming range,” *IEEE Photon. Technol. Lett.*, vol. 26, no. 5, pp. 465–468, Mar. 2014.
[12] S. H. Lee, K. Ahn, and J. K. Kwon, “Multilevel transmission in dimmable visible light communication systems,” *J. Lightw. Technol.*, vol. 31, no. 20, pp. 3267–3276, Oct. 2013.
[13] J.-N. Guo, J. Zhang, Y.-Y. Zhang, L. Li, Y. Zuo, and R.-H. Chen, “Multilevel transmission scheme based on parity check codes for VLC with dimming control,” *Opt. Commun.*, vol. 467, 2020, Art. no. 125733.
[14] L. Yi and S. G. Lee, “Performance improvement of dimmable VLC system with variable pulse amplitude and position modulation control scheme,” in *Proc. Int. Conf. Wireless Commun. Sensor Netw.*, Dec. 2014, pp. 81–85.
[15] A. Nuwanpriya, S. Ho, and C. S. Chen, “Indoor MIMO visible light communications: Novel angle diversity receivers for mobile users,” *IEEE J. Sel. Areas Commun.*, vol. 33, no. 9, pp. 1780–1792, Sep. 2015.
[16] H. Cai, J. Zhang, Y. Zhu, J. Zhang, and X. Yang, “Optimal constellation design for indoor 2×2 MIMO visible light communications,” *IEEE Commun. Lett.*, vol. 20, no. 2, pp. 264–267, Feb. 2016.
[17] T. Uday, A. Kumar, and L. Natarajan, “Low papr coding scheme for uniform illumination in MIMO VLC,” in *Proc. IEEE Globecom Workshops*, 2018, pp. 1–6.
[18] U. Thummaluri, A. Kumar, and L. Natarajan, “MIMO codes for uniform illumination across space and time in VLC with dimming control,” *IEEE Photon. J.*, vol. 11, no. 3, Jun. 2019, Art. no. 7903721.
[19] J.-H. Yoo, “Modelling and analysis of m-ary variable pulse position modulation for visible light communications,” *IET Optoelectronics*, vol. 9, pp. 184–190(6), Oct. 2015.
[20] *IEEE Recommended Practices for Modulating Current in High-Brightness LEDs for Mitigating Health Risks to Viewers*, IEEE Standard 1789-2015, pp. 1–80, 2015.
[21] X. Deng, K. Arulandu, Y. Wu, S. Mardanikorani, G. Zhou, and J. M. G. Linnartz, “Modeling and analysis of transmitter performance in visible light communications,” *IEEE Trans. Veh. Technol.*, vol. 68, no. 3, pp. 2316–2331, Mar. 2019.
[22] Z. Li, H. Yu, B. Shan, D. Zou, and S. Li, “New run-length limited codes in on-off keying visible light communication systems,” *IEEE Wireless Commun. Lett.*, vol. 9, no. 2, pp. 148–151, Feb. 2020.
[23] T. Uday, A. Kumar, and L. Natarajan, “Improved run length limited codes for VLC using dimming control compensation symbols,” in *Proc. 10th Int. Conf. Commun. Syst. Netw.*, Jan. 2018, pp. 457–460.
[24] Y. Zuo, J. Zhang, Y. Zhang, and R. Chen, “Weight threshold check coding for dimmable indoor visible light communication systems,” *IEEE Photon. J.*, vol. 10, no. 3, Jun. 2018, Art. no. 7904811.
[25] Y. Zuo and J. Zhang, “Joint data transmission and dimming control optimization for MIMO-VLC systems with channel-adaptive spatial constellation design,” *Opt. Commun.*, vol. 436, pp. 21–25, Apr. 2019.